MATLAB/SIMULINK MODELING OF MULTIPORT DC-DC CONVERTER

Mihai MIHĂESCU[1] Mihai Octavian POPESCU[2]

In recent decades the fields of use for multiport converters have known a significant expansion starting from applications in energy unconventional conversion up to the uses in the design and operation of hybrid and electrical motor vehicles. Driven by practical needs, a wide variety of topologies and ways of operation of these types of multiport converters have been studied, designed and made. This article presents MATLAB/SIMULINK model of an uninsulated DC-DC multiport converter with four ports: three inputs and one output for hybrid motor vehicles. The utility of this approach consists in the possibility to carry out studies regarding the efficiency and the operating modes.

Keywords: modeling, MATLAB/SIMULINK, multiport converter, simulation, uninsulated multiport converter

1. Introduction

At present, the use of renewable energy sources is continually growing. For this reason, remarkable progress has been registered in recent years in the development of technologies from the field of system that use the energy of wind, photovoltaic sources, fuel cells, biogas to enumerate just a few of them. Once highlighted the advantages of using them, the issue of their interfacing in order to obtain unique sources, regardless of the number of primary sources simultaneously delivering energy to the consumer (network or bus), has come up.

Despite the fact that, initially, when obtaining electricity from renewable sources the issue of interfacing several inputs appeared and was solved, once with the evolution of hybrid and electrical motor vehicles the issue of interfacing several outputs has come up. One of the ways of interfacing several inputs and several outputs is represented by the use of multiport DC-DC converters. An exhaustive analysis has been recently presented by Mojtaba Forouzesh and others in [1].

The first interfacing systems used in the technologies for the production of electricity from renewable sources were made of conventional configurations [2] which consisted in the use of several DC-DC converters, one for each energy

[1] PhD student, Faculty of Electrical Engineering, University POLITEHNICA of Bucharest, Romania, e-mail: mihaescumihai84@yahoo.com

[2] Prof., Faculty of Electrical Engineering, University POLITEHNICA of Bucharest, Romania

source, and the outputs of these converters were connected to a common DC network. This common network supplied a DC-AC converter for usual consumers.

Multiport DC-DC converters have shortly become an alternative for the interfacing of several renewable energy sources [3], [4], [5], [6], [8].

A multiport converter has more inputs and outputs connected to the respective DC-DC converter. Each DC-DC converter is then connected to a global element for energy storage unlike other separate elements for energy storage connected to the same network (conventional topology). The control of each DC-DC converter is made by a controller to control the power taken over from every input.

Taking into account the numerous topologies in case of hybrid vehicles where there are several inputs/outputs [5], in the following lines we will analyse an uninsulated DC-DC multiport converter with for ports. The skeleton diagram of such a multiport converter that is going to be modeled in Matlab/Simulink environment is given in Fig. 1.

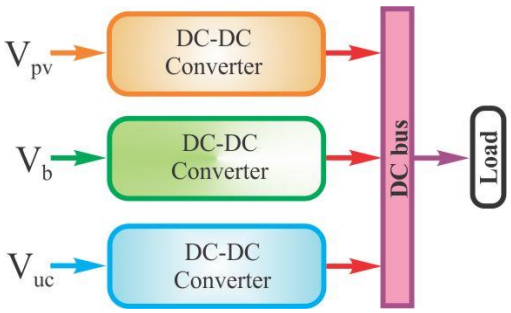

Fig. 1. Four ports non-isolated DC-DC converter block diagram.

2. Modeling and simulation of a four-port DC-DC converter for electric motor vehicles

Electric vehicles (EV) have become more and more popular due to the fact that they use green energy sources and function with zero toxic emissions. Initially, EVs were supplied from a single energy source such as the fuel cell or the storage battery [7]. Each of these sources has a maximum efficiency in different areas of operation. The EV supplied from a battery has a superior efficiency as compared to that supplied from the fuel cell. This has led to the development of the hybrid electric vehicles (HEV). Such a vehicle is supplied from two or more sources existing on board. Initially, HEV was designed to diminish the size of internal combustion engine. The evolution of HEV technology includes in its configuration the existence of several supply sources

and storage devices, as they may have any combination of photovoltaic cells, batteries, ultracapacitors, fuel cells, etc.

In the configuration of multiport converter presented by Santhosh and Govindajaru in [7] considered as referential, MOSFET transistors have been replaced by IGBT transistors to provide better versatility to the diagram and a higher level of originality to this paper. The modeled configuration is given in Fig. 2.

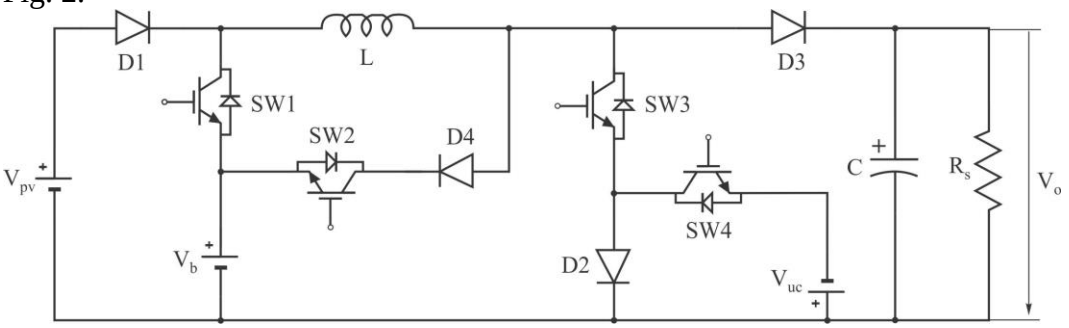

Fig. 2. Four port non-isolated DC-DC converter structure [7].

MATLAB/SIMULINK model of the four-port DC-DC converter relies on the configuration presented in Fig. 2. This converter represents the uninsulated version of a multiple input power electronic converter (MIPEC) [7]. The supply sources taken into account in this case are a photovoltaic panel (Vpv), a storage battery (Vb) and an ultracapacitor (Vuc).

The functioning of this converter requires the presence of some initial preloading levels. The storage battery and the ultracapacitor are considered to have been preloaded from an external source (in our case, the photovoltaic panel) up to a pre-established necessary level and aims to supply the DC bus of the vehicle control device with a constant voltage [7].

Matlab/SIMULINK model for the configuration of the converter under analysis is presented in Fig. 3.

The operating modes are dependent on the state of conduction and blocking of IGBT static contactors. Five operating modes may be identified in the operation of the converter according to the electric energy circulation.

Mode 1. Input source (Vpv) supplies directly the charge (the charge is resistor Rs in case of the model above).

Mode 2. The storage battery supplies the charge.

Mode 3. The input source and the ultracapacitor supply directly the charge.

Mode 4. The storage battery and the ultracapacitor supply the charge.

Mode 5. The input source charges the storage battery.

Mode 1. In this operating mode, the power taken over from the supply source V_{pv} (photovoltaic panels) is transmitted to the charge. Since static contactors have two states, conduction and blocking, the operation of the converter in each operating mode is studied according to the state of static contactors.

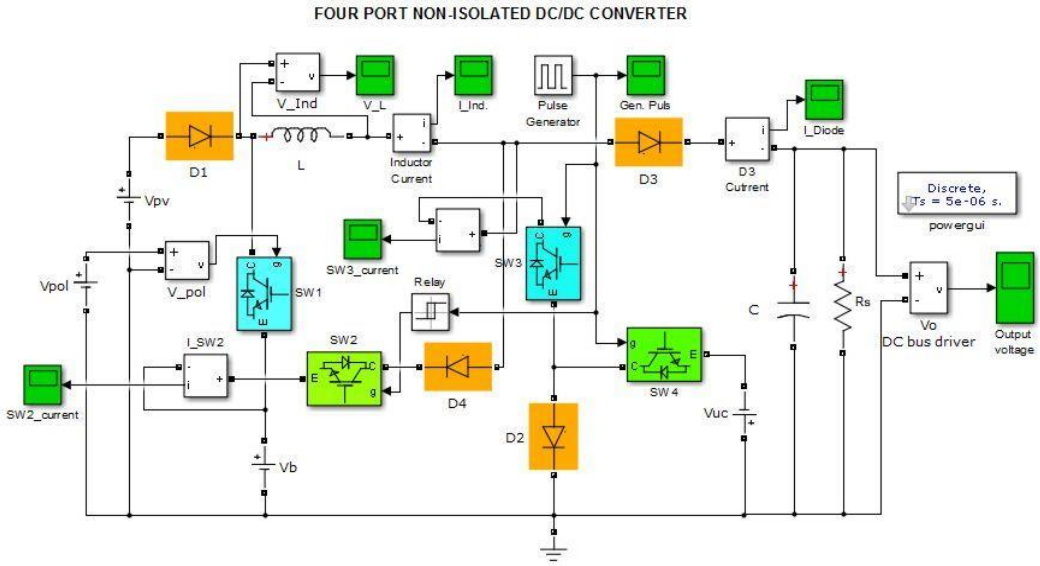

Fig. 3. Four ports non-isolated DC-DC converter MATLAB/SIMULINK model

M 1. Conduction state (*I*) detailed in Fig. 4. SW3, D1 and D2 are in conduction (ON) while inductance L absorbs current from the source.

The current absorbed from the source increases linearly:

$$\frac{di_L}{dt} = \frac{V_{pv}}{L} \quad . \tag{1}$$

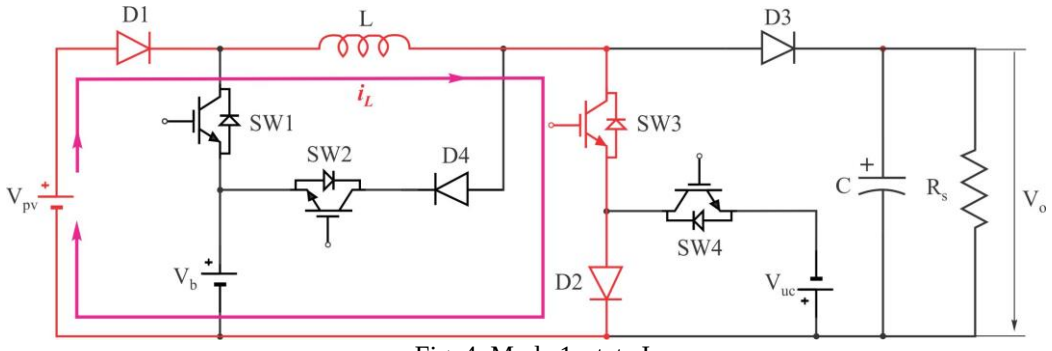

Fig. 4. Mode 1, state I.

M 1. Blocking state (*II*) is detailed in Fig. 5. SW3 is OFF while D1 and D3 are ON. The current runs from source V_{pv} and inductance L to charge R_s.

The current decreasing speed i_L is given by the formula:

$$\frac{di_L}{dt} = \frac{V_{pv} - V_o}{L} \ . \tag{2}$$

In the case in which we consider that the circuit operates in uninterrupted current regimen, when applying the theorem of volt-second balance (flow conservation) in terms of inductance L, it results:

$$V_L = V_{pv} - V_o(1 - D_c) = 0 \ , \tag{3}$$

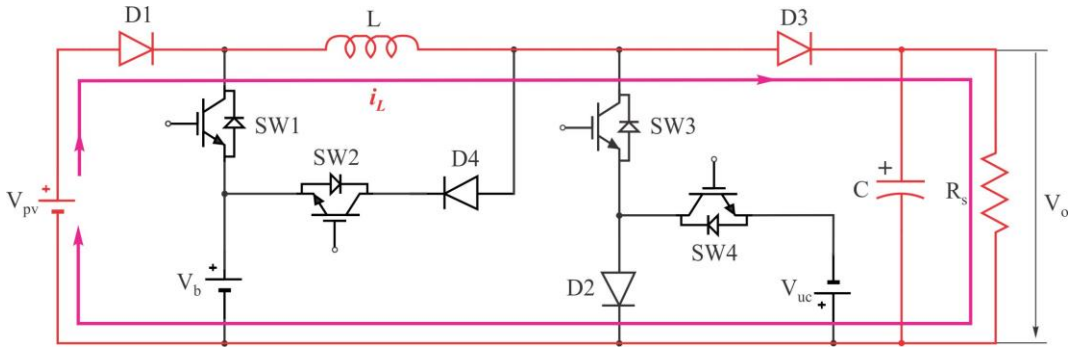

Fig. 5. Mode 1, state II.

where D_c is the relative conduction period or filling factor $D_c = \frac{t_{on}}{t_{on} + t_{off}} \cdot 100$ of contactor SW3 (in our case it has the value of 25%). In these conditions, it results that:

$$V_o = \frac{V_{pv}}{1 - D_c} \ . \tag{4}$$

Fig. 6 presents the evolution of voltage over time from the output of the converter on charge and current through diode D1.

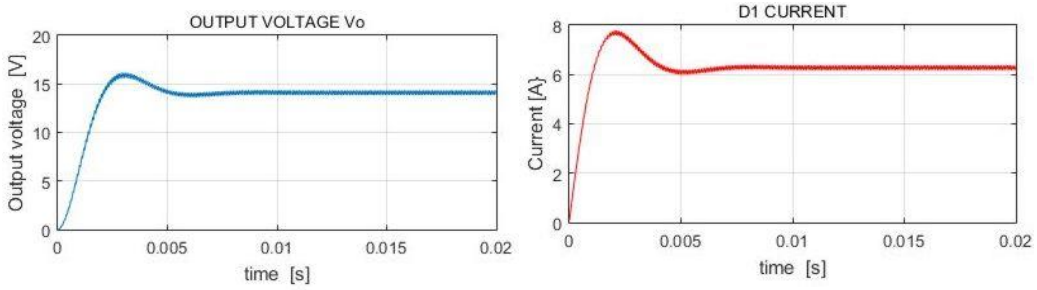

Fig. 6. Evolution of voltage over time from the output of the converter on charge and current through diode D1.

The values of these parameters correspond to a voltage V_{pv} = 12 V and a D_c factor of 25% of the gate drive pulses for contactor SW3. Voltage at charge terminals stabilize at the value V_0 = 14 V, and the absorbed current is I_{D1} = 6.3 A. By running the simulation, we may notice, as expected, that for a constant input voltage and the same value of charge R_s, the output voltage increases proportionally with D_c factor.

The signals characteristic to Operating mode 1 are given in Fig.7.

Mode 2. In this operating mode, the charge is supplied from the battery V_b = 12 V.

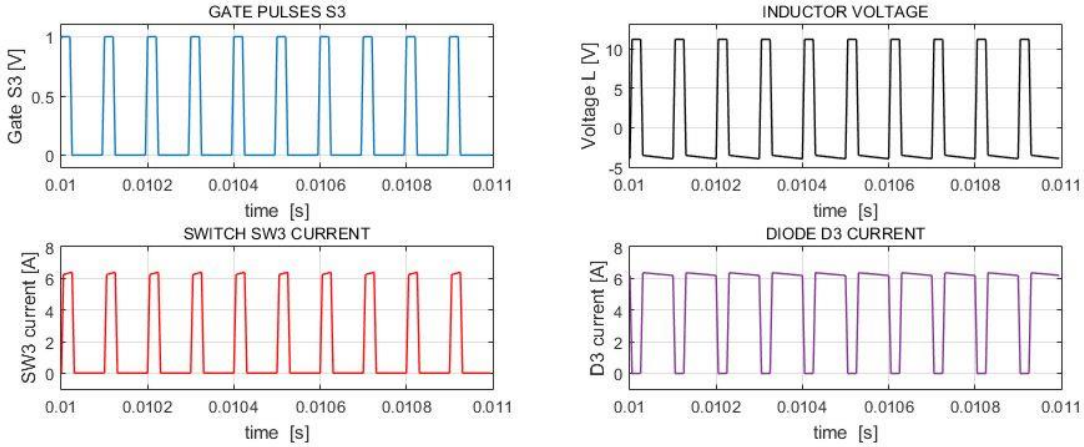

Fig. 7. The signals characteristic to Operating Mode 1.

M 2. State I (illustrated in Fig. 8). SW1, SW3, and D2 are ON, and inductance L absorbs current from the battery – the current increases linearly:

$$\frac{di_L}{dt} = \frac{V_b}{L} \quad . \tag{5}$$

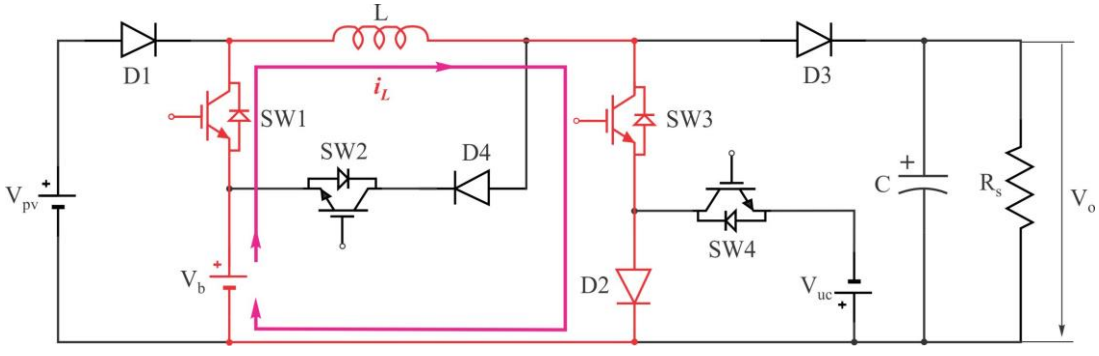

Fig. 8. Mode 2, state I.

M 2. State II (illustrated in Fig. 9). SW1 and D3 are ON and the charge is supplied from the battery by means of inductance L.

The current decreasing speed is given by the equation:

$$\frac{di_L}{dt} = \frac{V_b - V_o}{L} . \tag{6}$$

From the conditions of volt-second balance in relation to inductance L, it results:

$$V_o = \frac{Vb}{1 - D_c} . \tag{7}$$

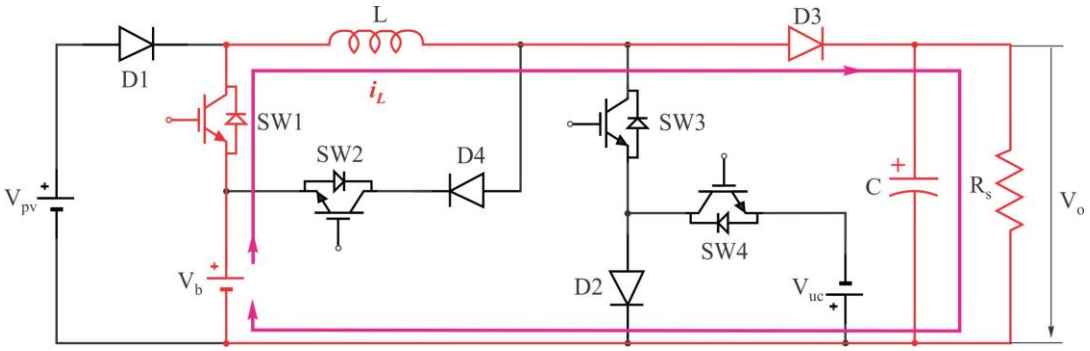

Fig. 9. Mode 2, state II.

Since in this operating mode contactor SW1 is ON for both states of contactor SW3, its gate was polarized from a continuous voltage source V_{pol} keeping it ON as long as the voltage value V_{pol} exceeds B-E voltage for the firm opening of the contactor throughout this operating mode. Since the static contactor SW1 is an IGBT transistor, the value V_{pol} = 1V was considered as sufficient. For the value V_b = 12 V and the same filling factor of 25%, the values of the output voltage and of the absorbed current are about the same with those in Fig. 6.

Source V_{pol} does not appear in the skeleton diagram et in the electronic diagram because in these diagrams there is no element of the command and control structure of the static contactors. But, in Matlab/Simulink model we need to show the Pulse Generator together with the Relay inversor which controls the static contactors (and which gives the possibility to modify D_c parameter), and V_{pol} polarization voltage of contactor SW1. We adopted this solution so as to be able to use the same force structure for all the operating modes. The change of the operating mode is also made by the modification of voltage value V_{pol} which equals 1 V only for Modes 2 and 4 while for the other modes it is null (SW1 is OFF). In conclusion, V_{pol} together with the Pulse Generator and the Relay are elements of the control circuit and are not elements of the force structure, a reason

for which they do not appear in Fig. 1 and Fig. 2. Fig. 10 presents the signals characteristic to this sequence.

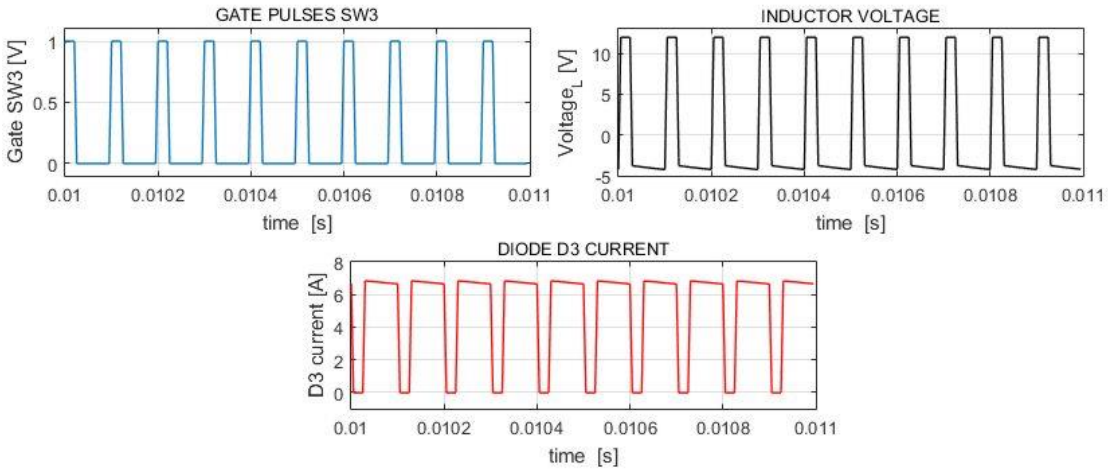

Fig.10. The signals characteristic Modului 2.

Mode 3. This operating mode is characteristic to the case when the source voltage V_{pv} decreases below a certain threshold value what implicitly leads to the decrease of output voltage V_0. To compensate the decrease of voltage, we introduce the ultracapacitor into the circuit while V_{pv} remains the main energy source.

M 3. State I (detailed in Fig. 11). D1, SW3 and SW4 areON. The circuit closes by inductance L absorbing energy.

The current increasing speed by inductance L is given by the equation:

$$\frac{di_L}{dt} = \frac{V_{pv} + V_{uc}}{L} \quad . \tag{8}$$

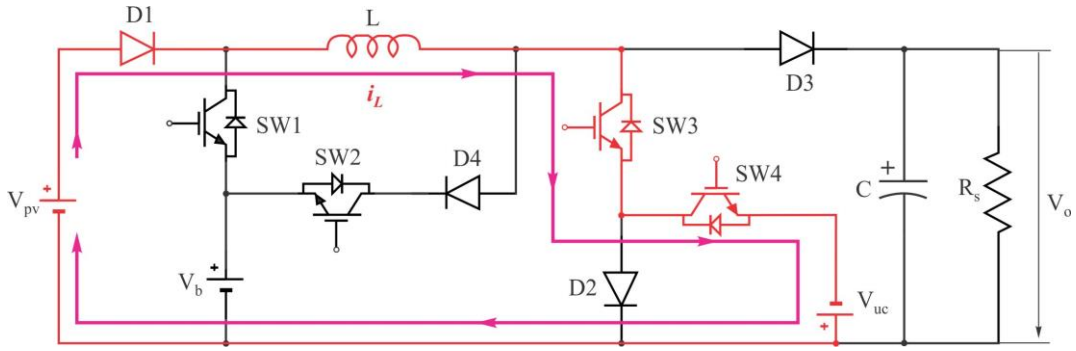

Fig. 11. Mode 3, state I.

M 3. State II (detailed in Fig. 12). D1 and D3 are ON. The accumulated energy is transferred to the charge and the inductance current evolves according to the equation:

$$\frac{di_L}{dt} = \frac{V_{pv} - V_o}{L} . \tag{9}$$

From the condition of volt-second balance for inductance L, it results that:

$$V_L = V_{pv} + D_c \cdot V_{uc} - V_o(1 - D_c) = 0 , \tag{10}$$

from where results:

$$V_o = \frac{V_{pv} + D_c \cdot V_{uc}}{1 - D_c} . \tag{11}$$

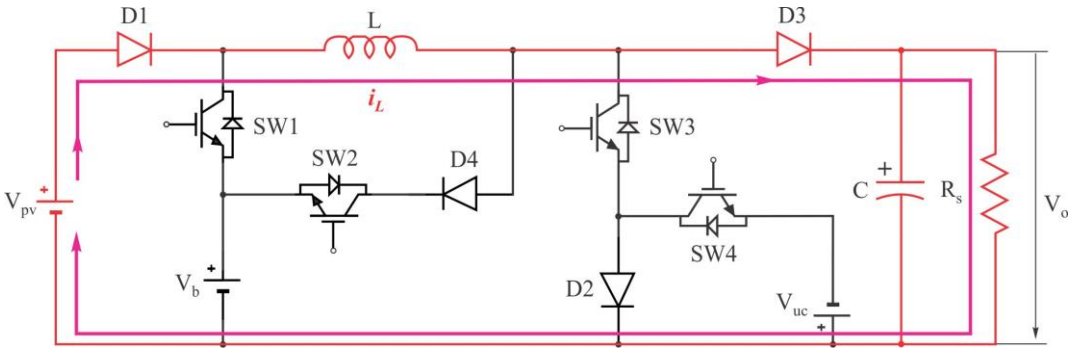

Fig. 12. Mode 3, state II.

Fig. 13 presents the signals characteristic of this operating mode.

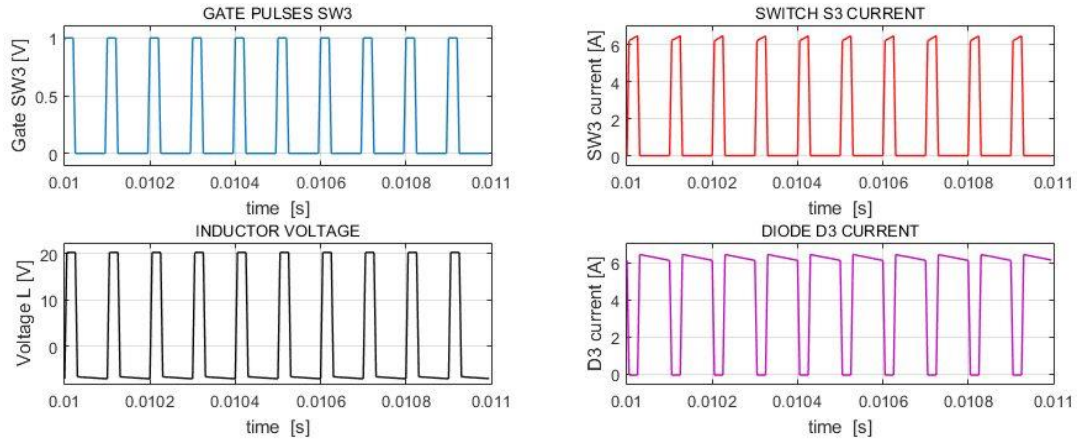

Fig.13. The signals characteristic Modului 3.

The results in Fig. 13 were obtained for an output voltage identical to that in Fig. 6, in the case when V_{pv} = 9 V, V_{uc} = 12 V and V_{pol} = 0, because SW1 is blocked.

Mode 4. In this operating mode, the ultracapacitor fulfils the same role in relation to the battery that it fulfilled in relation to the V_{pv} source in mode 3.

M 4. State I (Fig. 14). SW1, SW3 and SW4 are in conduction.

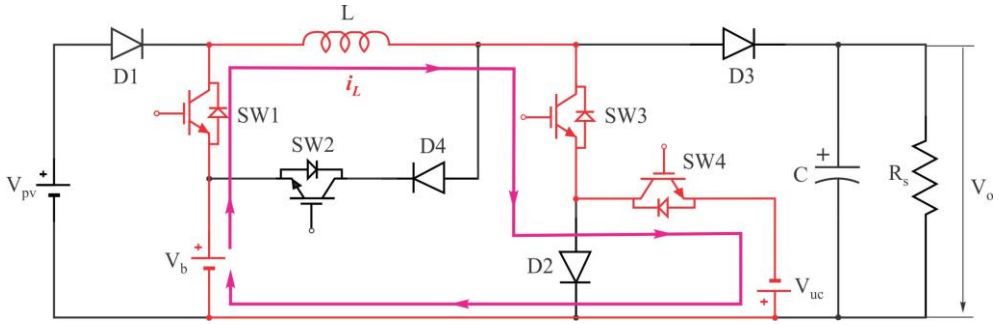

Fig. 14. Mode 4, state I.

M 4. State II (Fig.15). SW1 and D3 are in conduction.

The equations for the inductance current are identical to those in equations (8) and (9), except that voltage V_{pv} is replaced by the battery voltage V_b. After applying the flow conservation theorem, we finally obtain:

$$V_o = \frac{V_b + D_c \cdot V_{uc}}{1 - D_c} \ . \tag{12}$$

The results are identical to those obtained in operating mode 3, with the only difference that the role of source V_{pv} is taken by the storage battery (V_b).

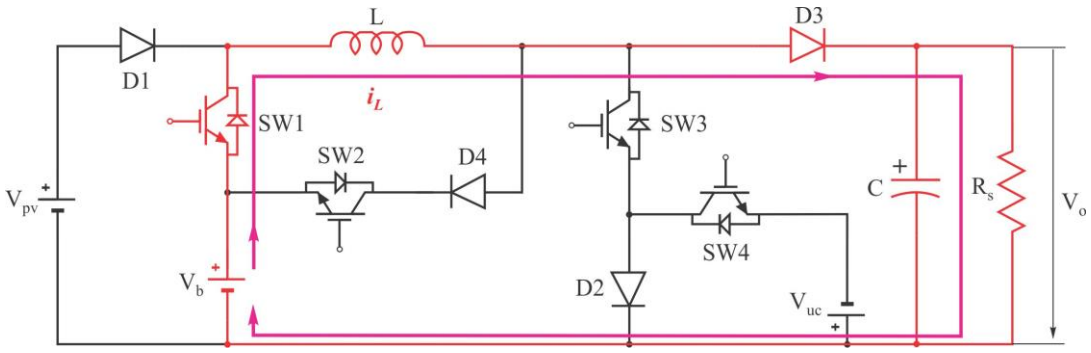

Fig. 15. Mode 4, state II.

The representative signals for operating mode 4 are given in Fig. 16.

Mode 5. In this case the battery is charged from the input source V_{pv}. This happens when the vehicle is placed at rest and PV panels generate energy. The energy excess generated by the photovoltaic panels when the vehicle is placed at rest is used to charge the battery.

M 5. State I (Fig. 17). SW3, D1 and D2 are in conduction.

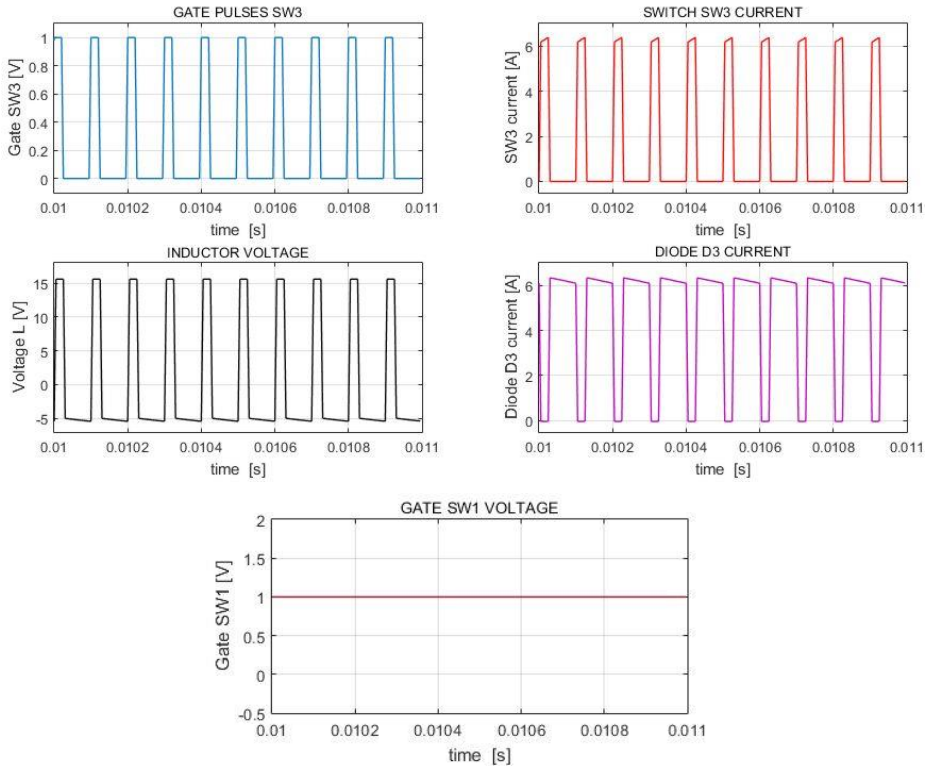

Fig. 16. The signals characteristic Modului 4.

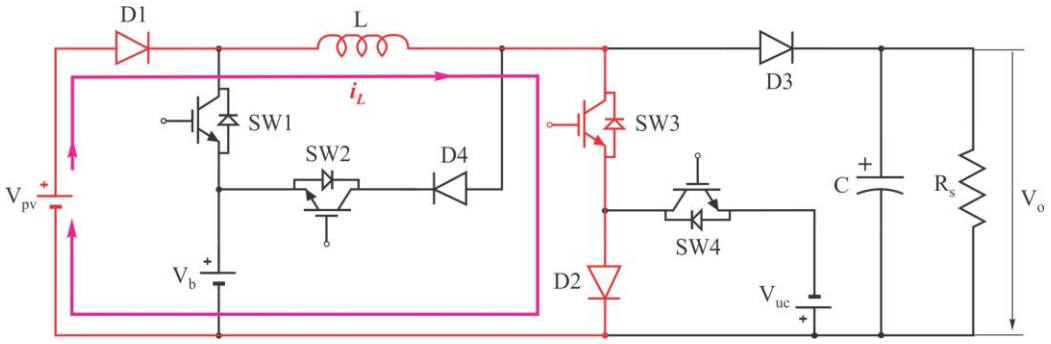

Fig. 17. Mode 5, state I.

M 5. State II (Fig. 18). SW2, D1 and D4 are ON. As we may see, the conduction states of contactors SW2 and SW3 are complementary. After applying the flow conservation theorem, in a stationary process, the voltage at battery terminals will have the formula:

$$V_b = \frac{V_{pv}}{D_c} . \tag{13}$$

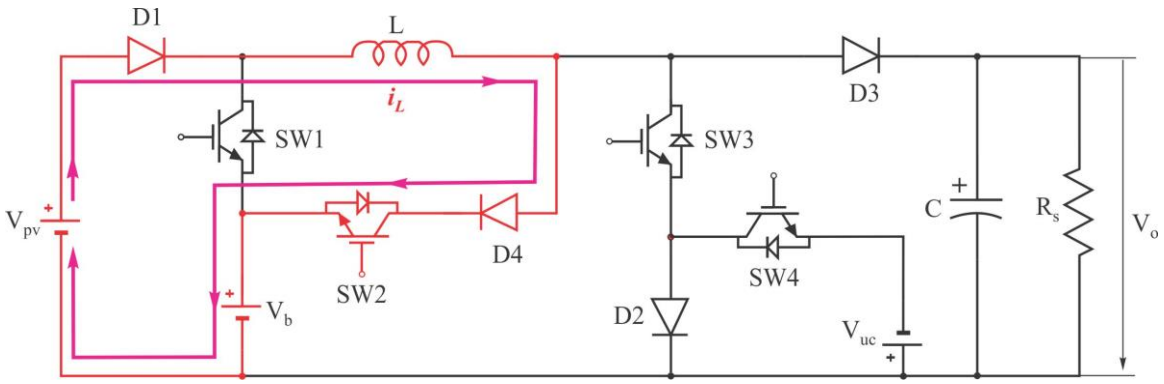

Fig. 18. Mode 5, state II.

The evolution over time of the parameters characteristic to this operating mode is given in Fig. 19.

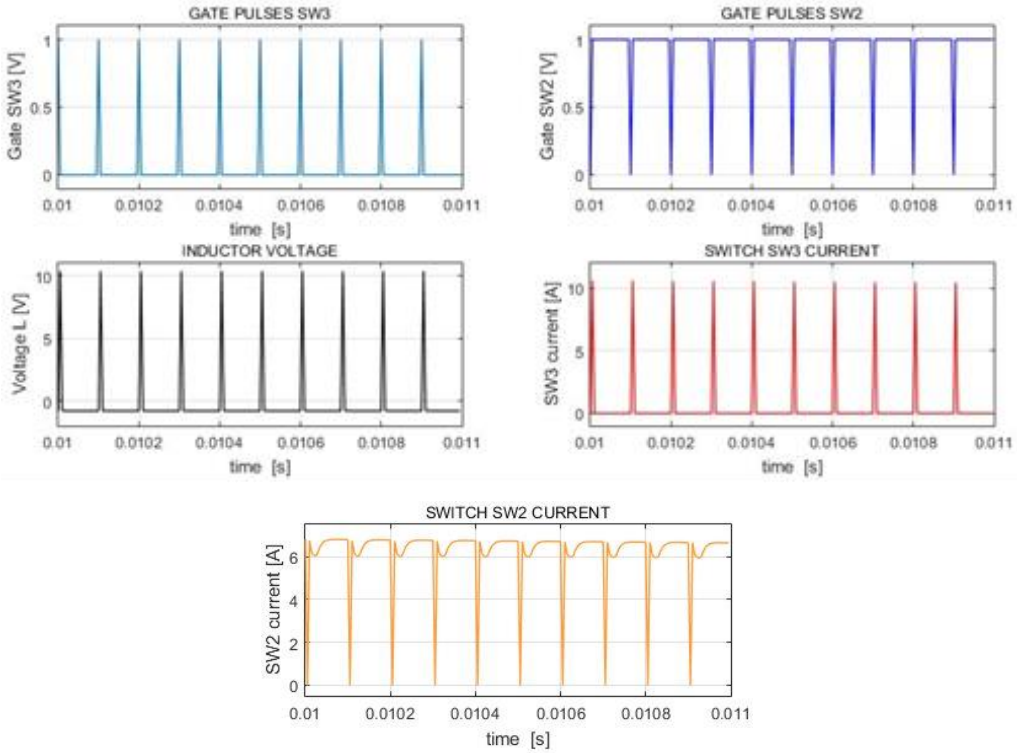

Fig. 19 The signals characteristic Modului 5.

The results of simulation of operating mode 5 were obtained in conditions where the photovoltaic panel voltage V_{pv} = 12 V, battery voltage V_b = 6 V, and the filling factor of control pulses (Dc) for SW3 was imposed to be 5% (according to Fig. 19). Since voltage sources in the model are considered to be ideal (zero internal resistance) and in order to have results of the study as close to reality as possible, we considered that in this operating mode the source modeling the battery V_b. is connected in series with a resistor 1 Ω (Fig. 20).

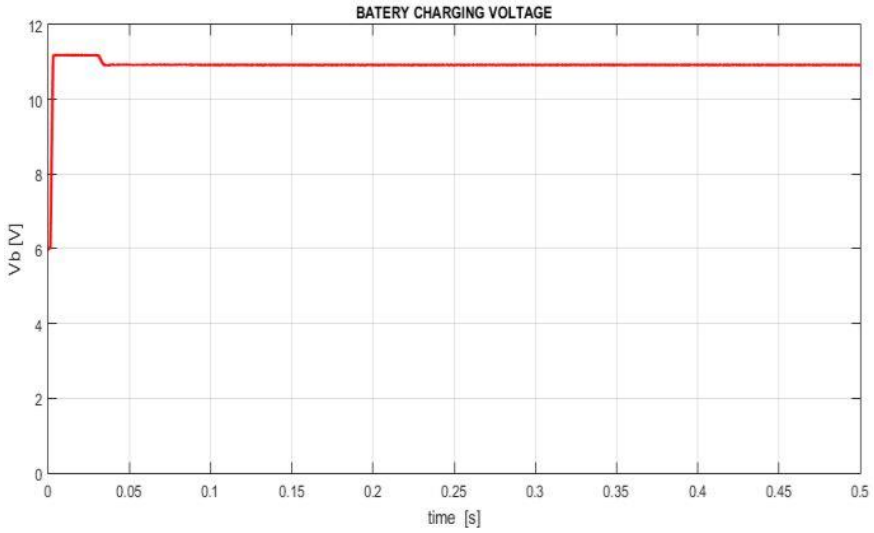

Fig. 20. Battery charging voltage.

3. Conclusions

The modeling of four-port converter to be used in the field of hybrid motor vehicles in MATLAB/SIMULINK environment allow us to obtain a versatile and flexible model as compared to those obtained by means of the applications specialized in the analysis and simulation of electronic circuits (ISIS Proteus). The model made by the author is more complex and allows the simulation and study of all operating modes (Mode 1 – Mode 5) for which the uninsulated converter with three inputs and one output proposed by Santhosh and Govindaraju was designed, both in stationary process and in transient state.

A significant advantage of modeling and simulating electronic circuits in toolbox Simscape (SimPowerSystems) of SIMULINK environment is the possibility to represent graphically, in a varied and friendly form, the evolutions of sizes characterizing the functioning of the circuit in a certain operation phase.

Authors chose for MATLAB/SIMULINK modeling the configuration given in [7], by taking into account the following considerations:

- The number of static contactors used in the 5 operating modes is reduced as compared to other configurations having the same number of inputs and outputs.
- Consequently, the structure of the command and control diagram will be simpler.
- The configuration allows us to charge the battery from an already existing source (V_{pv}). No additional source with the afferent converter is necessary to charge the battery (primary power source).
- Authors considered that this is a versatile configuration with a low number of static contactors that requires a simpler structure of the command and control system.

The model may be considered more complex than the configuration in [7] if we take into account the presence of control elements (Pulse Generator, Relay, V_{pol}) in the model, elements that do not appear in the diagram in Santhosh's paper.

R E F E R E N C E S

[1]. *Mojtaba Forouzesh, YamP. Siwakoti, Saman A. Gorji, Frede Blaabjerg and Brad Lehman*, "Step-Up DC–DC Converters: A Comprehensive Review of Voltage-Boosting Techniques, Topologies, and Applications", IEEE Transactions on Power Electronics, vol. 32, no. 12, pp. 9143-9178, dec. 2017.

[2]. *H. Tao, A. Kotsopoulos, J.L. Duarte, and M.A.M. Hendrix*, "Family of multiport bidirectional DC–DC converters," IEE Proceedings of Electric Power Applications, vol. 153, no. 3, pp. 451-458, May 2006.

[3]. *Mihai Mihăescu*, "Multiport Converters – a brief review", ECAI 2014 - International Conference – 7th Edition Electronics, Computers and Artificial Intelligence, 25 June -27 June, 2015, Bucharest, ROMÂNIA.

[4]. *Y.M. Chen, Y.C. Liu, S.C. Hung, and C.S. Cheng*, "Multi-input inverter for grid connected hybrid PV/wind power system," IEEE Transactions on Power *Electronics*, vol. 22, no. 3, pp. 1070-1077, May 2007.

[5]. *J.G. Kassakian, H.C. Wolf, J.M. Miller, and C.J. Hurton*, "Automotive electrical systems circa 2005," *IEEE Spectrum*, vol. 33, no. 8, pp. 22-27, Aug. 1996.

[6]. *H. Tao, A. Kotsopoulos, J.L. Duarte, and M.A.M. Hendrix*, "Multi-input bidirectional DC-DC converter combining DC-link and magnetic-coupling for fuel cell systems," in Proc. 40th Annual Meeting Industry Applications Conference, vol. 3, Oct. 2-6, 2005, pp. 2021-2028.

[7]. *T.K.Santhosh, C. Govindaraju*, "Simulation and Analysis of a Four Port DC/DC Converter for Hybrid Electric Vehicle", Power and Energy Systems: Towards Sustainable Energy (PESTSE 2014), 13-15 March 2014, Bangalore, India.

[8]. *I. Husain*, "Analysis and Design of a High-Power DC-DC Converter", M.S. Thesis, Texas A&M University, College Station, 1989.

[9]. *Brian R. Hunt Ronald L. Lipsman Jonathan M. Rosenberg*, "A Guide to MATLAB for Beginners and Experienced Users", Cambridge University Press, 2001, http://shrahroodud.ac.ir.pdf.

[10]. ***. "Simulink User's Guide", The MathWorks, Inc. 3 Apple Hill Drive 1999-2015, https://fenix.tecnico.ulisboa.pt/downloadFile/845043405443232/sl_using_r2015a.pdf.